SIAM J. APPL. MATH.
Vol. 0, No. 0, pp. 000–000

FROM LIFE-SAVING TO LIFE-THREATENING: A MATHEMATICAL MODEL TO SIMULATE BACTERIAL INFECTIONS IN SURGICAL PROCEDURES*

J. A. FERREIRA†, PAULA DE OLIVEIRA†, P. M. DA SILVA‡, AND M. GRASSI§

Abstract. Following the implantation of indwelling medical devices, bacteria inoculated during the surgery or coming from a preexistent focus of infection race for the medical surface where they attach. Adaptation to survive is a common feature of life, and microorganisms are not an exception. Bacteria form, in short periods of time, a habitat—the biofilm—where they develop multiresistance and tolerance to antibiotics and to the host immune system. To avoid its formation, researchers in the biomedical sciences showed evidence that coating medical devices with antibacterial agents—antibiotics—is a promising strategy. We present a mathematical model to simulate the action of an antibiotic, released from a medical surface, to fight bacterial infection. The model is composed by a system of partial differential equations that describe the distribution of drug and the evolution of a bacterial population. The preexistence of infection focus, the inoculation of bacteria during the surgery, the race for the medical surface, the resistance and tolerance of the population are taken into account. Analytical estimates of the bacterial density show the crucial importance of aseptic surgical procedures and of timely detection of preexisting infection focus. Numerical simulations illustrate several scenario.

Key words. bacterial growth, antibiotic action, PDE system, estimates, numerical simulations

AMS subject classifications. 35K10, 35Q92

DOI. 10.1137/20M1369610

1. Introduction.

Bacteria exist in two phenotypes: single cells that float in fluids or aggregates surrounded by a protective matrix. This habitat is generally referred to as the biofilm. What drives bacteria to form a biofilm? When bacteria aggregate, they have a larger likelihood to survive. In fact if an antibacterial drug permeates a biofilm, it would need a much larger amount of antibiotic than to eliminate the same density of planktonic bacteria. Moreover, within a biofilm, bacteria are more protected against the host immune system.

Bacteria can exhibit two different forms of decreased susceptibility: resistance and tolerance. All bacteria phenotypes—planktonic or biofilm—can become resistant, but only bacteria in biofilms exhibit tolerance. Resistance occurs when bacteria acquire genetic mutations, while tolerance is a transient variation that occurs when a population attains a certain density in an aggregate. Bacteria in biofilms exhibit 10–1,000 times more antibiotics tolerance than the planktonic cells ([20]). Therefore, once a biofilm forms, eradication of bacteria becomes a very difficult process.

Development of biofilms proceeds through different steps (Figure 1): attachment, growth, and dispersion. Biofilm formation generally implies the attachment to a biotic or an abiotic surface. For this reason the insertion of permanent or temporary medical devices increases enormously the risk of bacterial infections. The attraction of bacteria to attach to a surface—that some authors in the biomedical sciences call

*Received by the editors September 28, 2020; accepted for publication (in revised form) February 22, 2021; published electronically DATE.
https://doi.org/10.1137/20M1369610
†CMUC-Department of Mathematics, University of Coimbra, Coimbra, Portugal (ferreira@mat.uc.pt, poliveir@mat.uc.pt).
‡Instituto Politécnico de Coimbra, ISEC, DFM, Rua Pedro Nunes, 3030-199 Coimbra, Portugal. CMUC (pascals@isec.pt).
§Department of Engineering and Architecture, Trieste University, Trieste, 34127 Italy (mario.grassi@dia.units.it).

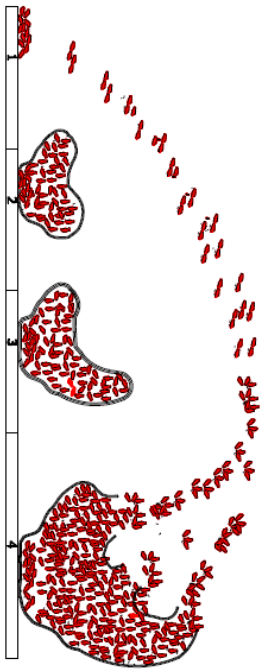

FIG. 1. *Biofilm formation.*

"the race for the surface"—can occur very fast, from some seconds to a few minutes. The formation of a biofilm is a slower process and typically can take some days.

With the constant increase of the number of medical implantable devices, biofilm formation of harmful bacteria on medical surfaces has become a worldwide and severe problem. As reported in [8] "about half of all nosocomial infections are associated with indwelling devices." Examples of infections involving surfaces can occur in the case of devices inserted into the human body for short periods of time, such as, for example, catheters and contact lenses, or in the case of medical devices that are meant to remain in place permanently, as artificial heart valves, cardiovascular stents, orthopedic implants, breast implants, or teeth implants. These implantable devices, that in some cases are life-saving, can become then a life-threatening risk.

There are three reasons that explain the occurrence of these postsurgical infections: the inoculation of bacteria during the surgery, the existence of focus of infection in the patient, or the simultaneous action of these two causes. As a result of the enormous difficulty in fighting infections once a biofilm develops—consequence of the multiresistance of bacteria and essentially of its ability to tolerate antibiotics and the defense mechanisms of the host immune system—it is crucial to avoid its formation. Due to the increasing role played by indwelling medical devices in monitoring and treatment, and the correlated threat of bacterial infections, researchers of different fields are studying antibiofilm strategies. Several antibiofilm approaches can be found in the biomedical literature as drug eluting coatings and surface alterations of medical devices. These alterations make difficult the attachment of bacteria and can be mechanical—for example, related to the rugosity of the surface—or chemical if they involve the treatment with chemical agents that prevent bacteria from binding to the surface. There is extensive literature on the topic, and we mention without being exhaustive [10], [18], and [31].

The sustained delivery of antibacterial drugs, dispersed in the surface of medical devices, is one of the strategies that can have a central role in the prevention

of hospital-acquired infections. In fact combining devices with the elution of a drug has shown to improve the efficacy by reducing the number of bacterial infections [15] and [19]. The idea has become so powerful that the World Health Organization has proposed, in 2019, a wider definition of medical device, which explicitly recognizes it may be assisted by pharmacological means in its primary functions. However large multi-institutional studies to select the optimal strategies are still lacking. While there is huge disciplinary research in different scientific domains dealing with the problem—material science, pharmacology, microbiology, and infectiology—an integrated multidisciplinary approach is missing in the literature.

Many questions do not have a clear answer by now. What is the real efficacy of the strategy? How does the success of in situ delivery depend on the extension and topology of surgical contamination? How does remote body infections influence the fate of the surgery? To take a step forward a mathematical approach of the problem can provide researchers with useful information to assist laboratorial and clinical studies. Currently to ensure the safety and the efficacy of a biomedical product it must be tested in vivo. However, clinical trials rarely tell us the reason why a product fails and how to improve it ([32]). In silico trials, allowing safe simulation even in extreme scenario—as (1) and (2) below—can provide a plethora of suggestions that help to reduce animal and human experimentation.

We present a mathematical model that simulates the interplay between a drug eluted from a medical device and the occurrence of an infection process caused by the simultaneous action of

1. Preexistent infection focus with different severities;
2. Bacterial inoculation during the surgery;
3. The "race for the medical surface";
4. The formation of a biofilm;
5. Resistance and tolerance of bacterial populations.

From a mathematical point of view, the model is represented by a system of coupled partial differential equations. The equations describe the release of an antibacterial drug from a surface coating of a medical indwelling device and the evolution of a bacterial population composed by planktonic and bacterial aggregates. The bacterial evolution is governed by a reaction-convection-diffusion equation that takes into account the random motion of bacteria, their biased motion in presence of a medical device, the formation of biofilms, and the action of an antibacterial agent on a resistant and tolerant population. From a medical point of view, the model in this paper contributes to clarify the role of preexisting infections, even if located at different sites from where the surgery is done. It also explains the crucial need for absolute asepsis in surgical procedures. Namely, the model shows (i) the deleterious consequences of inoculation—inoculum size and topology—during surgical procedures and (ii) how a preexisting infection associated with surgical contamination can dictate the failure of a device implantation.

Several authors have studied mathematical models of bacterial growth. We mention, for example, the interesting papers [34] and [26] where the authors study the interplay between bacteria and nutrients. In these papers the effect of antibacterial agents is not taken into account. Moreover bacterial evolution is governed by ordinary differential equations, consequently no random nor biased motion is considered. The influence of random motility in the survival of a bacterial population is studied in [3]. Competition and coexistence were examined for two bacterial species in [8]. A mathematical analysis of bacterial growth in a porous media was recently presented in [25] and [9].

In two papers recently published by some of the authors, the simulation of bacterial evolution under the action of a drug was presented. In [6], an ordinary differential

equation describes the bacterial evolution. Therefore, no random motion nor biased motion was taken into account. In [11] bacterial growth is governed by a PDE, but only the random motion of bacteria is considered. To the best of our knowledge the novelty of the present approach is twofold. From the modeling point of view the study of the simultaneous effect of the properties of the polymeric coating, the pharmacokinetics of the drug, the bacterial inoculation during surgery, the preexistence of infection focus, the race for the surface, and the multiresistance and tolerance of the bacterial population once a biofilm forms; from the analytical point of view the establishment of estimates that in spite of being obtained by a classical approach give meaningful biological information. Namely, the upper bounds in the estimates depend on the type of bacterial population, the pharmacokinetics of the drug, the severity and topology of the ioculation, and the health conditions of the patient.

The paper contains 4 sections. Following this introduction, we present in section 2 the mathematical model adopted and the biological reasons underlying our choice. In section 3 we deduce a priori estimates for the norm of the bacterial density. In section 4 several numerical simulations illustrate the behavior of the model. Finally in section 5 we address some conclusions.

2. Mathematical model.

2.1. Preliminaries. We assume that some type of drug eluting medical device—temporary or permanent—has been implanted in a patient and that during the surgery, bacteria (in the operating room, on the patient skin, or on the medical device) are inoculated. Moreover, we consider the case of preexisting infection focus in the patient. In Figure 2 we exhibit the drug eluting surface and the adjacent tissues: $\overline{\Omega}_1$ stands for a biodegradable polymeric coating of a medical device and $\overline{\Omega}_2$ represents the adjacent tissue. Orange circles or semicircles represent the focus inoculated during the surgery. Blue arrows represent the preexisting infections, located at remote body sites. The cascade of phenomena that occurs is described by the permeation of the interstitial fluid in the porous biodegradable coating, the dissolution and diffusion of the solid drug in the coating and in the adjacent tissues, and the fight against the bacterial population.

Let Ω be a two-dimensional open domain and $[0,T]$ a time interval.

If $w : \overline{\Omega} \times [0,T] \to \mathbb{R}$ we represent by $w(t)$, for $t \in [0,T]$, the function $w(t) : \overline{\Omega} \to \mathbb{R}$ given by $w(t)(x) = w(x,t), x \in \overline{\Omega}$. The drug is initially dispersed in Ω_1 in the solid state. When it enters in contact with the interstitial fluid, that permeates the surrounding tissue Ω_2, it dissolves progressively, and the drug is delivered through the interface $\partial\Omega_{1,2}$. The boundary $\partial\Omega_{1,\ell}$ represents the interface between the polymeric coating and an indwelling medical device. We assume that there are no fluxes—of interstitial fluid, drug, or bacteria—through this boundary.

The unknowns of the model are the concentration of interstitial fluid c_ℓ, the concentration of the solid drug c_s, the concentration of dissolved drug c_d, and the density of the bacterial population c_b.

As mentioned in section 1, the race for the surface immediately occurs while biofilm formation is a slower process. The drug is released in situ; however, under certain conditions, a biofilm may form on the surface. We will assume that a biofilm forms when the density of bacteria, attached to a surface, exceeds a certain threshold. This situation can occur because the drug is leached from the surface on the surrounding tissues and its concentration is insufficient to prevent biofilm formation. The focus of infection displayed in Figure 2 can represent biofilms, when bacteria are attached to the surface $\partial\Omega_{1,2}$, with a concentration that has surpassed a certain threshold. Otherwise the focus of infection represent an aggregate of planktonic bacteria.

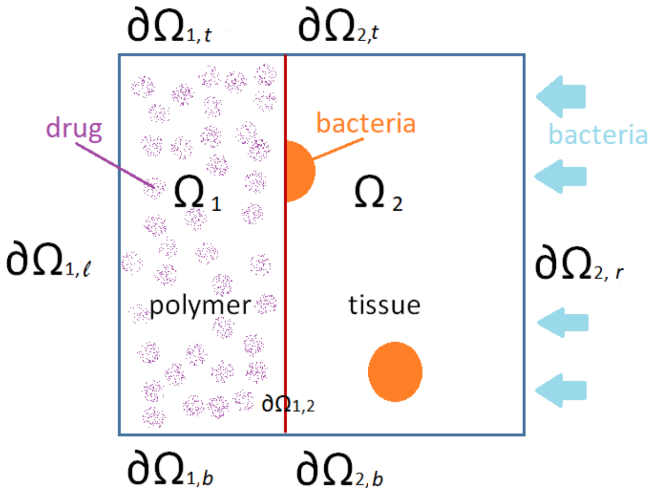

FIG. 2. *Spatial domain: the drug eluting coating is represented by Ω_1; the focus inoculated during the surgery are represented by orange circles or semicircles. A preexisting infection is signalized by blue arrows.*

The density of bacteria, c_b, is governed by

$$\frac{\partial c_b}{\partial t}(t) = \nabla \,.\, (D_b \nabla c_b(t)) + u \,.\, \nabla c_b(t) + F_b(c_d(t), c_b(t), t) c_b(t) \tag{1}$$

for $t \in (0, T]$, where the dissolved drug concentration in each domain is defined by $c_d = c_{d1}$ in Ω_1 and $c_d = c_{d2}$ in Ω_2. The diffusion coefficient D_b depends on space and is defined by

$$D_b(x) = \begin{cases} D_{b1}, & x \in \Omega_1, \\ D_{b2}, & x \in \Omega_2. \end{cases}$$

Regarding Brownian motion in (1), the random movement of microscopic objects in fluids caused by constant thermal agitation, is central in the microbial world ([5]). In the case of bacteria lacking mobility appendages, Brownian motion is, in part, responsible for facilitating movement. In the case of motile bacteria, Brownian motion can also affect deliberate movement, by randomizing displacement and direction ([17]).

There exists in the literature a large number of models to represent the race for the surface, that is, chemotaxis. One of the most known is the Keller–Segel model and its subsequent modifications ([33]). In the original model, chemotaxis is represented by a term of type

$$\nabla \cdot (\chi(s, c_b) c_b \nabla s),$$

where s stands for the chemoattractant density and χ is the chemotaxis response function. In the bacterial race for the surface, we assumed that ∇s and the response function are constants and consequently the term assumed a convection linear form. Moreover based on laboratorial studies we also assume that the race is convection dominated and orthogonal to the medical device surface (Figure 3). This justifies the rationale under a simplified definition of u : $u = (u_0, 0)$ in Ω_2. In Ω_1, the polymeric coating, we consider $u = (0, 0)$.

The net proliferation of bacteria is defined by

$$F_b(c_d, c_b, t) = E_0 \left(1 - \frac{c_b}{c_{b,max}}\right) - \frac{E_{max} e^{-\beta_b t} c_d^\gamma}{c_{50}^\gamma + c_d^\gamma}. \tag{2}$$

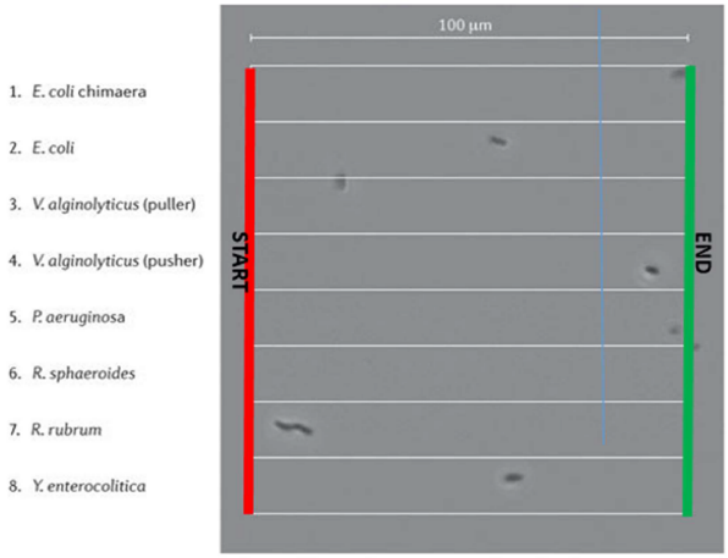

FIG. 3. *The Microbial Olympics—promoted by several research laboratories. Each cell type was recorded in a separate well and movies were combined afterwards. Adapted from* [33].

Equation (2) represents the balance between proliferation and the antibacterial action of the drug. The action of the drug is described by a generalization of the Hill model. This model is extensively used in the literature, and we believe that one of the reasons for its success is its flexibility and effectiveness in fitting experimental data ([13]). It includes the two main pharmacodynamic properties of a drug: the maximum effect (E_{max}) and the concentration producing 50% of the maximum effect (c_{50}). More precisely, E_{max} represents the maximum effect which can be expected from the drug, that is, the per capita death rate of bacteria due to the action of the drug at a certain concentration. When this magnitude of effect is reached, increasing the dose will not produce a greater magnitude of effect. In (2), γ is a shape parameter that represents a measure of the cooperation between bacteria. If $\gamma = 1$ the adhesion of the bacteria to the surfaces is independent of each other. If $\gamma > 1$, then there is cooperation, and if $\gamma < 1$ no cooperation occurs. The estimates for gamma depend on the specific drug. Different γ lead to significant differences in the steepness of (2). We will consider $\gamma = 1$. This value corresponds to the Hill coefficient presented in [4] for a particular strain of *Staphilococcus aureus* that colonize indwelling devices and a particular class of antibiotics.

Let us now address how tolerance and resistance influence (2). Tolerance occurs when a biofilm forms, that is, when a threshold bacterial density of an aggregate, attached to a surface, is achieved. As the biofilm matures tolerance increases. The term $e^{-\beta_b t}$ in (2) accounts for tolerance within the biofilm. The action of this exponential can be interpreted as a dramatic decrease of the maximum effect, E_{max}, once the biofilm forms. The first term in (2) represents the proliferation growth of the bacterial population by considering the carrying capacity of the environment, $c_{b,max}$, that depends on the availability of nutrients and oxygen. Although *Staphylococcus* species grow both aerobically and anaerobically, they grow best in an oxygen-rich environment. Resistance can be quantified via the pharmacodynamics of antibiotic action. One conventional measure of resistance is MIC (minimal inhibitory concentration). If we define MIC as the minimal concentration that inhibits bacterial net proliferation we have

$$MIC = c_{50}\left(\frac{E_{max}e^{-\beta_b t} - E_0}{E_0}\right)^{-\frac{1}{\gamma}},$$

that is, $MIC \geq c_{50}(E_{max} - E_0/E_0)^{-1/\gamma}$, where we assumed $c_{b,max}$ is not limited. For a constant γ, a larger MIC, that is, a larger resistance, can result from a larger c_{50} or a smaller E_{max} ([2]).

The behavior of the concentrations of the interstitial fluid, c_ℓ, the solid drug, c_s, and the dissolved drug, c_{d1}, in Ω_1, are governed by the following equations:

$$\begin{cases} \dfrac{\partial c_\ell}{\partial t}(t) = \nabla \,.\, (D_\ell(t)\nabla c_\ell(t)), \\ \dfrac{\partial c_{d1}}{\partial t}(t) = \nabla \,.\, (D_{ef}(t)\nabla c_{d1}(t)) + f(c_s(t), c_{d1}(t), c_\ell(t)) - R_{db}c_{d1}(t)c_b(t), \\ \dfrac{\partial c_s}{\partial t}(t) = -f(c_s(t), c_{d1}(t), c_\ell(t)) \end{cases} \tag{3}$$

for $t \in (0, T]$. In (3), D_ℓ represents the diffusion coefficient of the interstitial fluid in the polymeric coating. We consider that Ω_1 is a biodegradable porous medium able to host the interstitial fluid without undergoing a significant volume increase. This is the typical case of a polymer-matrix system characterized by a rheological behavior similar to that of a solid (elastic) material that never relaxes. In this case, indeed, despite solvent income, the polymeric network doesn't react. This means that the chains do not rearrange in space to host the solvent and that the reaction takes a long time. Consequently the solvent concentration will be always low and the volume increase is negligible. We also assume that D_ℓ is time dependent due to the time dependence of the biodegradable coating porosity. Accordingly the diffusion coefficient D_{ef} of the dissolved drug is also time dependent. For the time evolution of the porosity $\epsilon(t)$, due to the polymeric coating degradation, we consider ([34])

$$\epsilon(t) = \epsilon_0 + (1 - \epsilon_0)\left(1 + e^{-2k_d t} - e^{-k_d t}\right).$$

In this last expression ϵ_0 stands for the initial porosity of the polymeric coating and k_d represents the degradation rate. The effective diffusion coefficient of the interstitial fluid is represented by

$$D_\ell(t) = (\epsilon(t))^{\frac{3}{2}} D_{\ell,0},$$

where $D_{\ell,0}$ represents the initial diffusion in the nondegraded coating ([22]). In the previous definition we adopted the definition of effective diffusion as $\frac{\epsilon D}{\tau}$, where τ stands for the tortuosity, with $\tau = \frac{1}{\sqrt{\epsilon}}$. The diffusion coefficient of the dissolved drug is defined by

$$D_{ef}(t) = (\epsilon(t))^{\frac{3}{2}} D_1,$$

where D_1 stands for the drug diffusion coefficient in the nonhydrolyzed polymer.

Regarding the consumption term, $R_{db}c_{d1}c_b$, we observe that each class of antibacterial drug has a unique mode of action:

- It induces bacterial death by targeting the cell membrane of the bacteria (bactericidal). This type of drug prevents the bacteria from synthesizing a molecule in the cell wall, called peptidoglycan, which provides the wall with the strength it needs to survive in the human body;
- It slows or inhibits the growth of bacteria (bacteriostatic) by preventing key molecules from binding to selected sites on host cell structures, called ribosomes, where protein synthesis occurs. Without synthesis, bacteria can't reproduce or survive.

In the mathematical model presented in this paper, we describe these two different types of actions, from a macroscopic point of view, by considering that the drug acts by means of a sort of irreversible binding with the bacteria. Analogous representations are presented in [28] and [12]. The irreversible binding is represented by the term $R_{db}c_{d1}(t)c_b(t)$, where R_{db} stands for a positive constant. The reaction term f represents the rate of conversion of solid drug into dissolved drug and is defined by

$$f(c_s(t), c_{d1}(t), c_\ell(t)) = \alpha H(c_s(t))\frac{c_{sol} - c_{d1}(t)}{c_{sol}}c_\ell(t),$$

where α is the dissolution rate, H is the Heaviside function, and c_{sol} represents the solubility limit concentration ([27]).

The evolution of the dissolved drug concentration in Ω_2, c_{d2}, is described by

$$\frac{\partial c_{d2}}{\partial t}(t) = \nabla \cdot (D_{d2}\nabla c_{d2}(t)) - R_{db}c_{d2}(t)c_b(t) \tag{4}$$

for $t \in (0, T]$, where D_{d2} represents the diffusion coefficient. This coefficient is space dependent due to the fact that within biofilms diffusion coefficient has a lower value. Diffusion limitation occurs within a biofilm because fluid flow is reduced and the diffusion distance is increased. We define

$$D_{d2}(x) = \begin{cases} Tol, \ x \in \Omega_{2,b}, \\ D_{d2nob}, \ x \in \Omega_{2,nob} \end{cases}$$

with $Tol < D_{d2nob}$ and where $\Omega_{2,b}$ is the domain occupied by the biofilm and $\Omega_{2,nob} = \Omega_2 \backslash \Omega_{2,b}$. Regarding the biofilm formation we assume that it occurs once the bacterial density surpasses a certain threshold and when the agglomerate is attached to a surface.

Coupled systems (1), (3), (4) are completed with the following initial, boundary, and interface conditions:

- Initial conditions:

  $c_\ell(0) = c_{d1}(0) = 0$, $c_s(0) = c_{s,i}, c_b(0) = 0$ in Ω_1, $c_{d2}(0) = 0$, $c_b(0) = c_{b,i}$ in Ω_2.

  We note that the conditions related to solid drug, c_s, represent the fact that initially all the drug is in the solid state. The last condition represents the existence of an initial infection focus, consequence of surgical contamination.
- Boundary conditions:
  - $\partial\Omega_{1,\ell}$ is insulated; that is,

    $$J_c(t) \cdot \eta_1 = 0 \text{ on } \partial\Omega_{1,\ell}, \ t \in (0, T] \tag{5}$$

    for $c = c_i, i = b, \ell, d1$, where $J_{c_i}(t) = -D_i\nabla c_i$, $J_{c_{d1}}(t) = -D_{ef}\nabla c_{d1}$, and η_1 represents the unitary exterior normal to Ω_1. Condition (5) represents the case where the drug does not permeate the device. This situation can occur, for example, in the case of orthopedic implants.
  - on $\partial\Omega_{2,r}$

    $$J_{c_b}(t) \cdot \eta_2 = -\alpha_b c_{b,ext}(t) \text{ on } \partial\Omega_{2,r}, \ t \in (0, T], \tag{6}$$

    where, as before, $J_{c_b}(t) = -D_b\nabla c_b(t) - u_0 c_b(t)$, η_2 represents the unitary exterior normal to Ω_2, and $c_{b,ext}(t)$ represents an exterior bacterial concentration. The condition on $\partial\Omega_{2,r}$ for c_b describes a preexistent body infection focus (see Figure 2) with density $c_{b,ext}(t)$. If no preexistent infection exists, then we consider

    $$J_{c_b}(t) \cdot \eta_2 = 0 \quad \text{on } \partial\Omega_{2,r} \times (0, T]. \tag{7}$$

– symmetry conditions on $\bigcup_{i=1,2,j=t,b} \partial\Omega_{i,j}$ that are mathematically defined by

$$\frac{\partial c}{\partial x_2}(t) = 0 \text{ on } \bigcup_{j=t,b} \partial\Omega_{1,j}, t \in (0,T]$$

for $c = c_\ell, c_{d2}, c_b$, and

$$\frac{\partial c}{\partial x_2}(t) = 0 \text{ on } \bigcup_{j=t,b} \partial\Omega_{2,j}, t \in (0,T]$$

for $c = c_{d2}, c_b$.

- Interface conditions:
  On the common boundary of Ω_1 and Ω_2, $\partial\Omega_{1,2}$, we assume that the fluid flux is proportional to the difference between the fluid concentration on the boundary and the fluid concentration c_{ext} in Ω_2, that is, $J_{c_\ell}(t).\eta_2 = \varphi(c_\ell(t) - c_{ext})$ on $\partial\Omega_{1,2}, t \in (0,T]$, where φ is related with the permeability of the interface that, to simplify, we assume time independent. For the dissolved drug concentration we assume the continuity of the concentration and of the flux, that is,

$$c_{d,1}(t) = c_{d,2}(t),\ J_{c_{d1}}(t).\eta_1 + J_{c_{d2}}(t).\eta_2 = 0 \quad \text{on } \partial\Omega_{1,2},\ t \in (0,T].$$

For the bacterial density $c_b(t)$ on the interface $\partial\Omega_{1,2}$ we also assume

$$c_{b,1}(t) = c_{b,2}(t),\ J_{c_{b1}}(t).\eta_1 + J_{c_{b2}}(t).\eta_2 = 0 \quad \text{on } \partial\Omega_{1,2},\ t \in (0,T], \tag{8}$$

where $c_{b,i}$ denotes the bacterial density in $\Omega_i, i = 1,2$.

The assumptions on the continuity of drug concentration and drug flux at the interface are the simplest assumptions we can adopt. Indeed, possible concentration discontinuity at the interface is due to different thermodynamic environments on the two sides of the interface; also possible flux discontinuity should be motivated by the presence of particular phenomena such as chemical reactions on one or both sides of the interface. Although these phenomena could occur, we do not have clear evidences to sustain such hypotheses. Regarding interface conditions on bacterial density analogous comments could be done.

3. A priori estimates. In this section, we present a priori estimates of the bacterial concentration and the total bacterial mass, when an infection occurs, after a medical indwelling device is implanted. The mathematical proofs are included in section 6. The inclusion of those estimates has a twofold aim: to show the stability of the model and to illustrate that stability estimates can give insight on the solution behavior, namely, regarding its dependence on the parameters of the model. Two different situations are analyzed:

1. A contamination during the surgery;
2. The preexistence of a remote body site infection.

In what follows we estimate $\|c_b(t)\|_{L^2(\Omega)}$, with $\Omega = \Omega_1 \cup \Omega_2$, where $\|.\|_{L^2(\Omega)}$ denotes the usual norm in $L^2(\Omega)$ associated with the usual inner product $(.,.)_{L^2(\Omega)}$. We consider that the free drug concentration that arises in the definition of F_b in Ω_i has a lower bound $\overline{c}_{d,i}$, that is, $c_{d,i}(t) \geq \overline{c}_{d,i}$ in $\Omega_i, i = 1,2$. We also assume that $\partial\Omega_i$, $i = 1,2$, are counterclockwise oriented.

A contamination during the surgery.

Let us suppose that there is no remote infection and that the bacteria are inoculated at the initial time in the tissue or on the medical device. Then the behavior of $c_b(t)$ on $\partial\Omega_{2,r}$ is given by (7), that is,

$$J_{c_b}(t)\ .\ \eta_2 = 0 \,\text{on}\, \partial\Omega_{2,r} \times (0,T].$$

In this scenario the following result can be established.

PROPOSITION 3.1. *If $c_{d,i}(t) \geq \bar{c}_{d,i}$ in Ω_i, then for the bacterial density $c_b(t)$ defined by* (1) *and the boundary and interface conditions* (5), (6), *and* (7), *respectively, we have*

(9)
$$\|c_b(t)\|^2_{L^2(\Omega)} + 2\min\{D_{b1}, D_{b2}\}\int_0^t e^{2\theta(t-\mu)}\|\nabla c_b(\mu)\|^2_{[L^2(\Omega)]^2}d\mu \leq e^{2\theta t}\|c_b(0)\|^2_{L^2(\Omega)}$$

for $t \in [0,T]$. In (9), *θ is given by*

$$\theta = \max_{i=1,2}\left(E_0 - e^{-\beta_b T_f}E_{max}\frac{\bar{c}_{d,i}}{c_{50}+\bar{c}_{d,i}}\right). \tag{10}$$

Let $M_b(t)$ be the bacterial mass in Ω. As $M_b(t) \leq \sqrt{|\Omega|}\|c_b(t)\|_{L^2(\Omega)}$, where $|\Omega|$ denotes the measure of Ω, we easily get the following estimate.

COROLLARY 3.1. *Under the assumptions of Proposition* 3.1 *we have*

$$M_b(t) \leq \sqrt{|\Omega|}e^{\theta t}\|c_b(0)\|_{L^2(\Omega)}, t \in [0,T], \tag{11}$$

where θ is given by (10).

Given an upper bound ϵ_b for the bacterial mass in Ω, from Corollary 3.1 we easily compute a threshold time t^* such that for $t \leq t^*$ we have $M_b(t) \leq \epsilon_b$. In fact, it is sufficient to take

$$t^* = \frac{1}{\theta}\ln\left(\frac{\epsilon_b}{\sqrt{|\Omega|}\|c_b(0)\|_{L^2(\Omega)}}\right). \tag{12}$$

Moreover, if the drug effect dominates the bacterial growth rate, that is,

$$E_0 - E_{max}e^{-\beta_b T_f}\frac{\bar{c}_{d,i}}{c_{50}+\bar{c}_{d,i}} < 0, \tag{13}$$

then, from (11),

$$M_b(t) \to 0, t \to \infty. \tag{14}$$

Preexistence of a remote body site infection and contamination during the surgery.

PROPOSITION 3.2. *If $c_{d,i}(t) \geq \bar{c}_{d,i}$ in Ω_i, then for the bacterial density $c_b(t)$ defined by* (1) *and the boundary and interface conditions* (5), (6), *and* (8), *respectively, we have*

$$\begin{aligned}&\|c_b(t)\|^2_{L^2(\Omega)} + 2\min\{D_{b1}, D_{b2}-\delta^2 T_r\}\int_0^t e^{2\theta(t-\mu)}\|\nabla c_b(\mu)\|^2_{[L^2(\Omega)]^2}d\mu \\ &\leq e^{2\theta t}\|c_b(0)\|^2_{L^2(\Omega)} + \frac{\alpha_b^2}{2\delta^2}\int_0^t e^{2\theta\mu}\int_{\partial\Omega_{2,r\uparrow}} c_{b,ext}(\mu)^2 ds d\mu, t \in [0,T],\end{aligned} \tag{15}$$

where $\delta \neq 0$, θ is defined by (10) *and T_r is such that $\|w\|^2_{L^2(\partial\Omega_2)} \leq T_r\|w\|^2_{H^1(\Omega_2)}$ with $\|.\|^2_{H^1(\Omega_2)}$ denoting the usual norm in $H^1(\Omega_2)$.*

For the bacterial mass $M_b(t)$ we establish the following result.

COROLLARY 3.2. *Under the assumptions of Proposition* 3.2 *we have*

$$M_b(t) \leq \sqrt{|\Omega|}\left(e^{2\theta t}\|c_b(0)\|^2_{L^2(\Omega)} + \frac{\alpha_b^2 T_r}{D_{b2}}\int_0^t e^{2\theta\mu}\int_{\partial\Omega_{2,r\uparrow}} c_{b,ext}(\mu)^2 ds d\mu\right)^{1/2},$$

where θ is defined by (10) *and $t \in [0,T]$.*

The estimate in Corollary 3.2 is in agreement with biological evidence: The total mass of the bacterial colony increases with the severity of the infection and the amount of bacteria inoculated.

Under the assumptions of Proposition 3.2, if $c_{b,ext}(t)$ is bounded by $\hat{c}_{b,ext}$, then the bacterial mass satisfies

$$M_b(t) \leq \sqrt{|\Omega|}\left(\|c_b(0)\|_{L^2(\Omega)} + \alpha_b\sqrt{\frac{T_r}{D_{b2}}}\sqrt{\frac{|\partial\Omega_{2,r}|}{|\theta|}}\hat{c}_{b,ext}\right), t \geq 0,$$

provided that the drug effects $E_{max}e^{-\beta_b T_f}\bar{c}_{d,i}/c_{50} + \bar{c}_{d,i}$ exceeds the bacterial birth rate E_0.

The estimate in Corollary 3.2 is illustrated in Figure 10. The dependence of the total mass of bacteria on the severity of the remote body site infection, represented by $c_{b,ext}$, is illustrated in Figure 11.

4. Simulations. The problem was solved for the first 10 hours after surgery and considering different initial bacterial focus, using *comsol multiphysics* software. A quadratic piecewise finite element method for the concentrations is considered. A triangular mesh automatically generated with 38,940 elements is used to obtain a consistent mesh in the square domain $[0,5]\times[0,5]$. The time integration is performed with a backward difference method, with variable order ranging between 1 and 2 and an adaptative time step. We begin by presenting in subsection 4.1 the evolution of a bacterial population, after contamination during a surgical procedure. In subsection 4.2 the effect of a preexistent infection on the evolution of a bacterial population is analyzed. We also discuss the simultaneous effect of bacterial contamination and the preexistence of infection focus in the host.

We start by considering $\beta_b = 10^{-4}$ ((2)). We recall that the factor $e^{-\beta_b t}E_{max}$ represents the decrease of E_{max} that characterizes biofilm structures. It is activated only on the interface $\partial\Omega_{1,2}$ that stands for the surface of the medical device. This is a consequence of the fact that bacteria need to attach to a surface to form a biofilm. The activation takes place when the bacterial population attains a certain threshold, that is, when a biofilm is formed. In our simulations this threshold is $\bar{c}_b = 1$. All numerical results regarding bacterial distribution are represented in mol/m^3 and the masses in mol.

4.1. Evolution of a bacterial population after contamination during a surgical procedure. In this section we illustrate the evolution of a bacterial population when contamination takes place during a surgical procedure. The values in Table 1 are used in all the simulations. The pharmacodynamic parameters correspond to Daptomycin ([4]).

We begin by presenting in Figure 4 a global picture of the masses of interstitial fluid (M_ℓ), solid drug (M_s), and dissolved drug (M_d) in Ω_1 for an initial bacterial density $c_{i,b} = 5$. The mass of interstitial fluid increases over time until a steady state is reached. The mass of solid drug decreases as the interstitial fluid permeates the polymer and accordingly the mass of dissolved drug increases.

Contamination during a surgical procedure: The influence of the severity of contamination.

The distribution of the bacterial concentration for three different initial inoculations in the adjacent tissue is represented in Figure 5: $c_{i,b} = 5$ (i), $c_{i,b} = 50$ (ii), two focus, $c_{i,b} = 5$ and $c_{i,b2} = 10$ (iii). This last focus is attached to the interface $\partial\Omega_{1,2}$. The simulations are exhibited for $t = 20$ min, $t = 4$ h, and $t = 10$ h. In the three cases we observe a race of bacteria for the medical surface. On the left column, (i) with $c_{i,b} = 5$, the drug delivered from the medical device eliminates the infection; in

TABLE 1
Parameter values used in the numerical simulations.

Parameter (unit)	Value	Parameter (unit)	Value
$D_{\ell,0}$ (m^2/s)	10^{-9}	D_1 (m^2/s)	7.8×10^{-11}
D_2 (m^2/s)	$2D_1$	D_{d2nob} (m^2/s)	$4D_1$
D_{tol} (m^2/s)	$D_{d2nob}/2$	D_{b1} (m^2/s)	5×10^{-12}
D_{b2} (m^2/s)	5×10^{-11}	α $(1/s)$	10^{-4}
c_{50} (mol/mm^3)	0.5	c_{sol} (mol/mm^3)	2
$c_{s,i}$ (mol/mm^3)	5	c_{ext} (mol/mm^3)	1
$c_{b,max}$ (mol/mm^3)	500	γ	1
k_d	3×10^{-4}	ϵ_0	5×10^{-2}
β (m/s)	10^{-6}	L_1, L_2 (mm)	2, 3
k_1, k_2	0.1, 0.1	R_{db} $(m^3/(mol * s))$	5×10^{-5}
E_{max} (h^{-1})	3	E_0 (h^{-1})	0.9
u_0 (m/s)	5×10^{-7}		

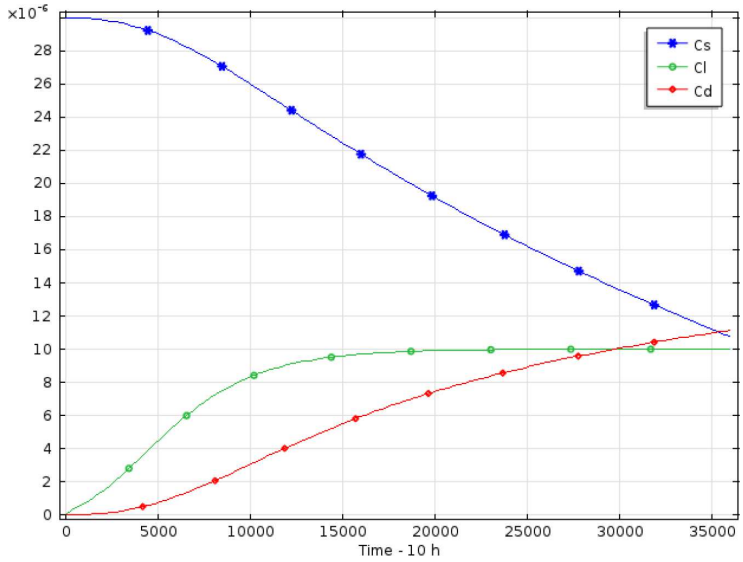

FIG. 4. *Behavior of masses of interstitial fluid, solid drug, and dissolved drug during* 10 *hours.*

the middle column, (ii) where $c_{i,b} = 50$, the drug delivered is not effective in fighting the infection; on the right column (iii) a second focus in the interface is added to case (i). In situations (ii) and (iii) biofilm formation is observed and the infection evolves out of control.

In Figure 6 the evolution of the bacterial mass during 10 hours is represented for $c_{i,b} = 5$, $c_{i,b} = 10$, and $c_{i,b} = 50$. Observing the three plots we conclude that there exists a threshold $c^*_{i,b}$ for the initial bacterial concentration such that there is an inversion in the evolution of the infection. For the data used in the simulations, $5 < c^*_{i,b} < 10$. For $c_{i,b} = 5$, it can be observed that 1.5 hours after the surgical procedure, the bacterial density decreases and the amount of bacteria is almost null after 6 h. In the case the initial inoculation during the surgical procedure is $c_{i,b} = 10$, 50, the drug eluted from the coating is not enough to fight the infection.

Contamination of the medical device and adjacent tissue: The influence of topology and location.

The dependence of the fate of the medical device on the degree of contamination, illustrated in Figures 5 and 6 is not a surprising result. In fact, it is expected that

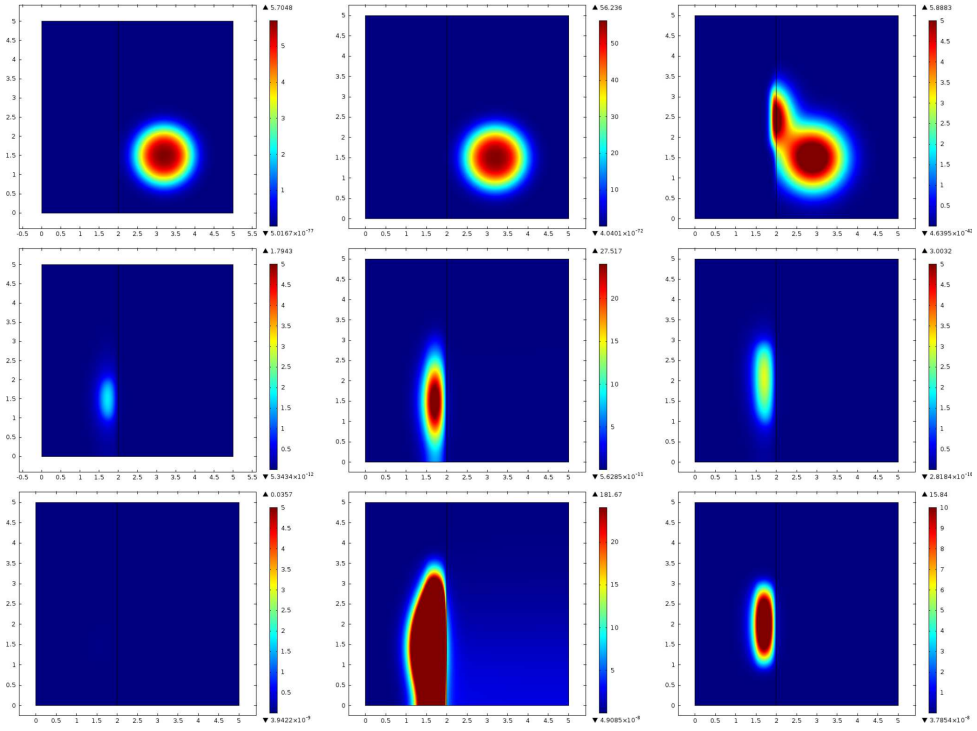

FIG. 5. *Bacterial distribution at* 20 *min (top),* 4 *h (middle), and* 10 *h (bottom):* (i) $c_{i,b} = 5$, *left;* (ii) $c_{i,b} = 50$, *middle and* (iii) *with* $c_{i,b} = 5$ *and* $c_{i,b2} = 10$, *right.*

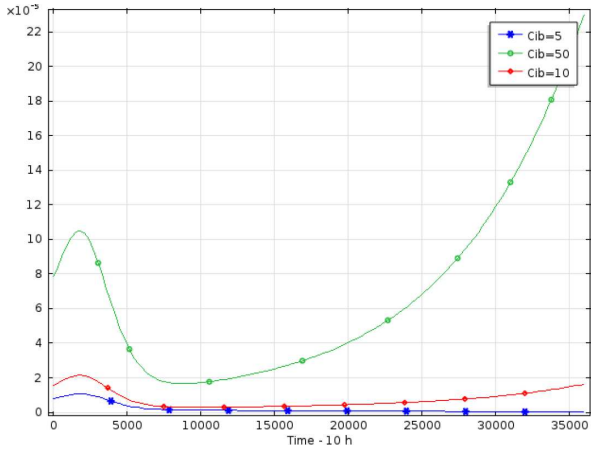

FIG. 6. *Evolution of the bacterial mass during* 10 *hours for* $c_{i,b} = 5$, $c_{i,b} = 10$, *and* $c_{i,b} = 50$.

a more severe initial contamination leads to an uncontrolled infection as established in section 3. The effect of the initial topology and location of the inoculation is less intuitive. How does this initial topology influences the evolution of the infection process? Does the location of initial contamination in the adjacent tissue matter? We consider three cases, represented in the schema of Figure 7, all of them with the same initial bacterial mass:

(i) one bacterial agglomerate with $c_{ib} = 10$ was inoculated during the surgical procedure;

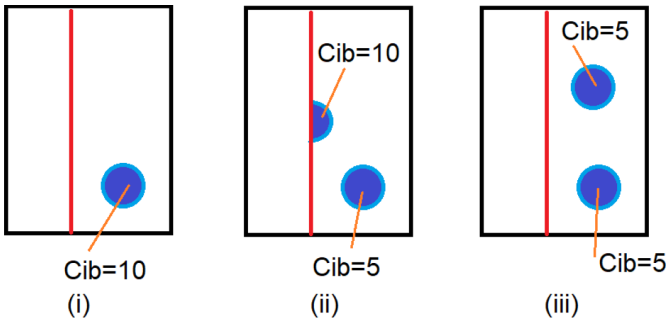

FIG. 7. *The initial topology of the contamination.*

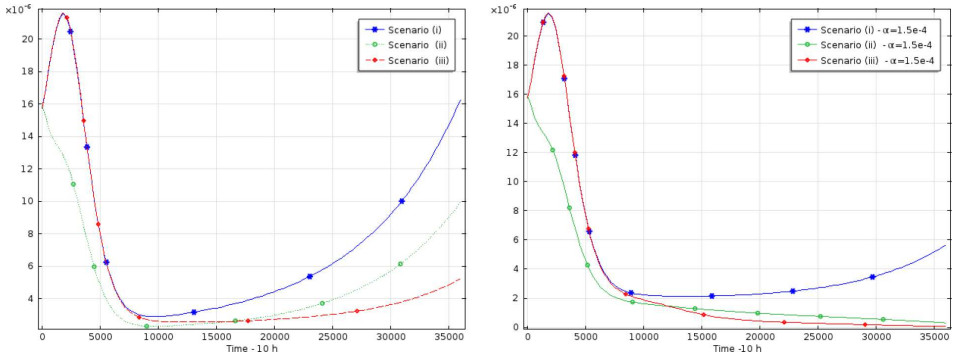

FIG. 8. *Bacterial mass in scenarios* (i), (ii), (iii) *of Figure* 7 *with* $\alpha = 10^{-4}$*—left;* $\alpha = 1.5 \times 10^{-4}$*—right. The total initial bacterial mass is the same in the three cases; the location and topology of the contamination is different.*

(ii) the medical device was contaminated with a focus of $c_{ib} = 10$ with a semi-circular geometry; moreover the adjacent tissue was also contaminated during the surgery with a focus of $c_{ib} = 5$;

(iii) two bacterial agglomerates with $c_{ib} = 5$ were inoculated in the adjacent tissue.

The initial total mass of bacteria is the same in the three cases. In Figure 8 we exhibit the evolution of masses in cases (i)—(iii). The surprising result is that although the initial bacterial mass is the same for the three scenario, the total mass of bacteria evolves differently.

In cases (i) and (iii) the plots have 3 phases: a first phase where the bacterial mass increases, because the drug molecules and the bacteria need a certain interval of time to meet; a second phase where the mass decreases due to the drug effect; a third phase where the bacterial mass increases because the available amount of drug is not enough to fight the infection. In case (ii) the focus with $c_{ib} = 10$ that occupies an half circle is on the medical interface (Figure 7); consequently, the drug molecules eluted from the surface immediately kick this interface agglomerate and the total mass of bacteria sharply decreases. In cases (i), (ii), and (iii) the last increasing phase suggests that the available drug is not enough to fight the infection (Figure 8(left)). In Figure 8(right) we illustrate the effect of the dissolution rate α that regulates the amount of available drug. While in the simulations of Figure 8(left) we use $\alpha = 10^{-4}$, in Figure 8(right) $\alpha = 1.5 \times 10^{-4}$. In this case the mass of bacterial drug evolves differently in the three scenarios. The illustrations in this subsection suggest that

- asepsis conditions of surgeries are crucial: the fate of the medical device depends on the severity of initial contamination;

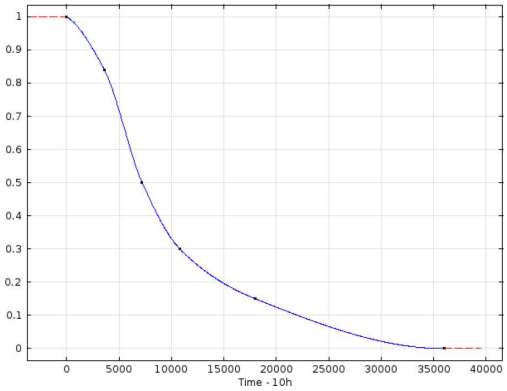

FIG. 9. *Behavior of the bacterial mass coming from a remote preexisting body site infection during* 10 *hours.*

- the contamination of adjacent tissues is harder to eliminate than the contamination located on the device.

4.2. Fate of the surgical procedure in presence of a preexisting remote body site infection. We will consider in what follows that the infection is not due to inoculation during the surgical procedure but to a preexisting infection focus. This preexisting infection focus is represented in the mathematical model by the boundary condition (6)

$$J_c(t) \,.\, \eta_2 = -\alpha_b c_{b,ext}(t) \text{ on } \partial\Omega_{2,r},\ t \in (0,T],$$

where $c_{b,ext}$ stands for the bacterial density of the remote preexisting focus.

It is assumed the remote infection is detected and therefore is being treated with an additional systemic antibacterial drug. The behavior of the mass of bacteria that reaches the boundary of the domain $\partial\Omega_{2,r}$ is represented in Figure 9.

In section 4.1 we have illustrated the influence of contamination during a surgical procedure; in section 4.2 we consider an aseptic surgical operating room but the existence of a remote site infection. A third situation is the simultaneous effect of in situ contamination during the surgical procedure and the preexistence of a remote body site infection. In Figure 10 we compare these three scenarios considering that the initial bacterial contamination is $c_{ib} = 5$ and that the concentration of the remote body site infection is represented in Figure 9. We conclude that, for the data used in the simulations, the drug release from the surgical device is effective in fighting the infection only in the case of device contamination.

We illustrate now the dependence of the bacterial population on some parameters of the model.

Bacterial concentration coming from a remote preexisting body- $c_{b,ext}$*.*

The influence of the bacterial concentration coming from a remote preexisting body site infection for two different magnitude is illustrated in Figure 11. As expected, a higher severity of the remote infection implies the presence of a larger amount of bacteria.

Tolerance: Activation level of β_b*.*

In Figure 12(left) is illustrated the behavior of the evolution of bacteria over 10 hours for different activation levels of the term β_b in (2). This term accounts for tolerance; that is, the ability of microorganisms to resist being killed by antibiotics. As biofilm forms, tolerance increases dramatically. We assume that biofilm forms on the interface polymer coating/tissue as the population density attains a certain

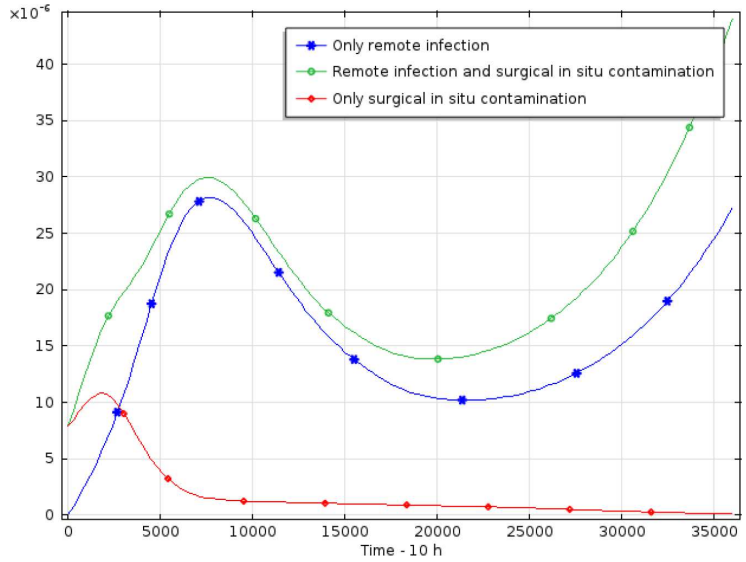

FIG. 10. *Bacterial mass during* 10 *h for: a remote body site infection, a remote body site infection and occurrence of contamination during the surgical procedure, a contamination during the surgical procedure.*

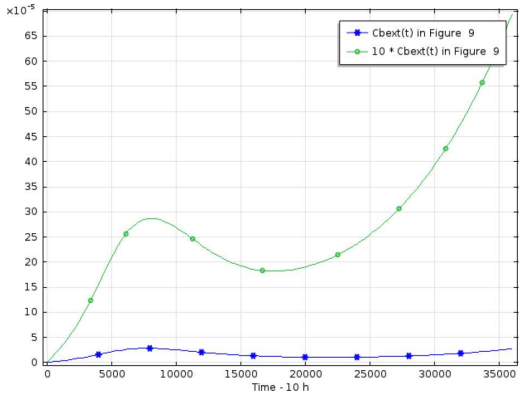

FIG. 11. *Behavior of the bacterial mass coming from a remote preexisting body site infection for two different magnitude during* 10 *hours.*

threshold. Two situations are simulated: the biofilm forms as the bacterial density is larger than $\bar{c_b} = 1$; the biofilm forms as the bacterial density surpasses $\bar{c_b} = 100$. It can be seen that the larger the density needed to form a biofilm is, the more efficient the antibacterial fight is.

The race for the surface: The convection rate of the population.

In Figure 12(right) $\bar{c_b} = 100$ is fixed and the dependence on the convection rate is analyzed. Three different values are considered $u_0 = 5\times10^{-7}$, 3×10^{-7}, and 2×10^{-7}. The bacterial density is a decreasing function of u_0. In fact when the population races for the surface, the bacteria kick the drug molecules: A small convection rate gives the colony a longer period to evolve before the action of drug is felt in the aggregate.

Resistance: E_{max} of the antibacterial drug.

As mentioned before, the antibiotic resistance can be simulated by decreasing E_{max}. The influence of E_{max} on the bacterial mass during 10 hours is represented in Figure 13—for $E_{max} = 3$, 30 and considering the biofilm forms as the bacterial

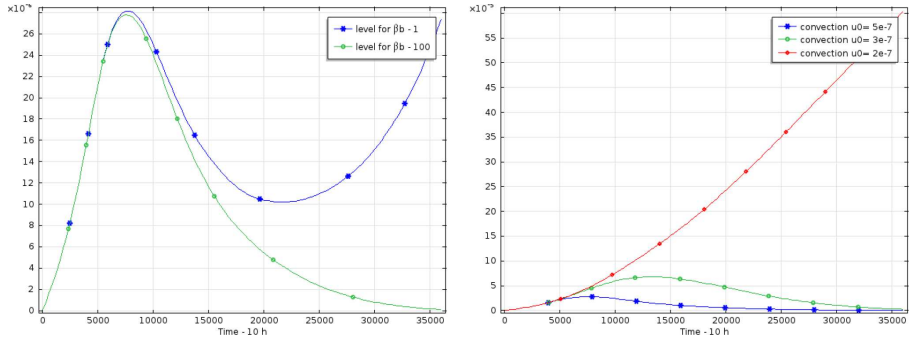

FIG. 12. *Comparison of the bacterial mass for two different minimal bacterial concentrations needed to form a biofilm—activation level of* β_b*:* $\bar{c_b} = 1$ *and* $\bar{c_b} = 100$*—left; influence of the convection rate when* $\bar{c_b} = 100$*—right.*

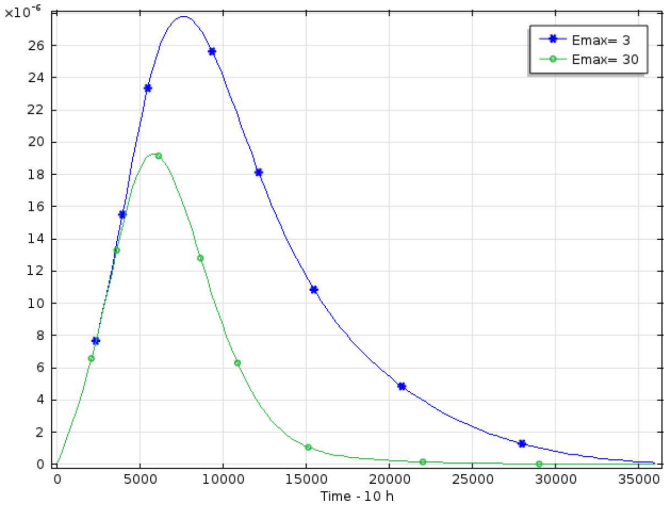

FIG. 13. *Influence of* E_{max} *on the bacterial mass during* 10 *h (with* $\bar{c_b} = 100$*).*

density surpasses $\bar{c_b} = 100$. We remark that this parameter is responsible for the efficiency of the drug in fighting the infection. As expected, an increase of E_{max} leads to a decrease of the bacterial mass along time.

5. Conclusion. The insertion of permanent or nonpermanent invasive medical devices is a common procedure in modern surgical practice. Diseases of all body systems take benefit of these procedures—from catheters to heart valves, cardiovascular stents, joint prostheses, therapeutic lenses, cochlear implants, ventricular assist devices, artificial hearts, or brain stimulators. However, the insertion of medical devices predispose to infection due to two main reasons: epithelial barriers are damaged with the surgical procedure and surfaces are a support for bacterial growth and biofilm formation. The most common cause of healthcare-associated infections can be attributed to indwelling medical devices. As a consequence, worldwide nosocomial infections represent a major public health problem. The sustained delivery of antibacterial drugs, dispersed in the surface of medical devices, is one of the strategies that can have a central role in the prevention of those hospital-acquired infections. Nonetheless, many questions do not have a clear answer by now. To move forward the debate, we present a mathematical model that governs the evolution of a bacterial population under the action of an antibacterial drug and assumes a surgery acquired infection and/or a

preexisting infection in the patient. We believe this viewpoint that has been adopted, regarding the in situ origin of the infection and/or a remote origin of the infection, represents a contribution to advance our understanding of the problem.

The present paper has a double character. An applied character as the numerical simulations provide some unexpected medical answers (sections 4.1 and 4.2) but also a theoretical character as we establish a priori estimates for the bacterial concentration and mass (section 3). These estimates exhibit upper bounds that provide meaningful biological information. In Proposition 3.1 (surgical inoculation), the upper bound represents a balance between the growth rate of the bacterial population, the action of the drug, and the severity of the inoculation. In Proposition 3.2 the severity of a preexistent infection appears as part of the balance.

Concerning the medical outcomes, we analyze three different scenarios:

1. Contamination during the surgical procedure;
2. Existence of a remote body site infection or postsurgical acquired infection;
3. Contamination during the surgical procedure and simultaneous existence of a remote body site infection or a postsurgical acquired infection.

Regarding 1, 2, and 3, our simulations suggest

- The severity of the postsurgical infection and the fate of the medical device depend on the degree of contamination of the indwelling device and the surgical procedure itself (Figures 5 and 6);
- The severity of the postsurgical infection and the fate of the medical device depend on the topology and location of the initial contamination (Figures 7 and 8);
- The local release of drug is more effective when a moderate contamination has occurred during the surgery; an infection in a remote body site or a postsurgery acquired hospital infection are not controlled by the local delivery even if a co-adjutant systemic antibiotherapy is used (Figure 10);
- The evolution of the infection depends on the threshold concentration the particular strain needs to form a biofilm (Figure 12(left));

We are aware that the problem of nosocomial infections is a complex one, involving a multidisciplinary approach and multiple factors. Obviously only some of those factors are considered in the model presented in the current paper. Consequently at the present stage, the model should be viewed as a proof of concept, describing a specific host–pathogen interaction. As the demand for indwelling medical devices is expected to continuously grow during the next decade due to the increasing use of minimally invasive surgeries, we trust now is the right time to study how concepts and prototypes of a certain number of indwelling devices can handle with bacterial infections.

6. Annex. Proof of Proposition 3.2.

In what follows we estimate $\|c_b(t)\|_{L^2(\Omega)}$, with $\Omega = \Omega_1 \cup \Omega_2$, where $\|.\|_{L^2(\Omega)}$ denotes the usual norm in $L^2(\Omega)$ associated with the usual inner product $(.,.)_{L^2(\Omega)}$.

We consider that the free drug concentration that arises in the definition of F_b in Ω_i has a lower bound $\overline{c}_{d,i}$; that is, $c_{d,i}(t) \geq \overline{c}_{d,i}$ in $\Omega_i, i = 1, 2$. We also assume that $\partial\Omega_i$, $i = 1, 2$, are counterclockwise oriented.

Preexistence of a remote body site infection.

From (1) in Ω_1 we deduce

$$\frac{1}{2}\frac{d}{dt}\|c_b(t)\|^2_{L^2(\Omega_1)} = -\int_{\partial\Omega_1} J_{c_b}(t).\eta_1 c_b(t) ds - D_{b1}\|\nabla c_b(t)\|^2_{[L^2(\Omega_1)]^2} + (F_b(t)c_b(t), c_b(t))_{L^2(\Omega_1)},$$

where $\|.\|_{[L^2(\Omega_1)]^2}$ denotes the usual norm in $[L^2(\Omega_1)]^2$ induced by the usual inner product $(.,.)_{[L^2(\Omega_1)]^2}$.

Using the boundary conditions on $\partial\Omega_{1,\ell}, \partial\Omega_{1,b}$, and $\partial\Omega_{1,t}$ we get

$$\frac{1}{2}\frac{d}{dt}\|c_b(t)\|^2_{L^2(\Omega_1)} = -\int_{\partial\Omega_{1,2\uparrow}} J_{c_b}(t).\eta_1 c_b(t)ds - D_{b1}\|\nabla c_b(t)\|^2_{[L^2(\Omega_1)]^2} + (F_b(t)c_b(t), c_b(t))_{L^2(\Omega_1)}. \tag{16}$$

From (1) in Ω_2 we establish

$$\frac{1}{2}\frac{d}{dt}\|c_b(t)\|^2_{L^2(\Omega_2)} = \int_{\partial\Omega_2} -J_{c_b}(t).\eta_2 c_b(t)ds - D_{b2}\|\nabla c_b(t)\|^2_{[L^2(\Omega_2)]^2} - (uc_b(t), \nabla c_b(t))_{[L^2(\Omega_2)]^2} + (F_b(t)c_b(t), c_b(t))_{L^2(\Omega_2)}.$$

From the symmetric boundary conditions for $c_b(t)$ on $\partial\Omega_{2,t}$ and $\partial\Omega_{2,b}$ we easily obtain

$$\frac{1}{2}\frac{d}{dt}\|c_b(t)\|^2_{L^2(\Omega_2)} = \int_{\partial\Omega_{1,2\downarrow}} -J_{c_b}(t).\eta_2 c_b(t)ds - \int_{\partial\Omega_{2,r\uparrow}} J_{c_b}(t).\eta_2 c_b(t)ds - D_{b2}\|\nabla c_b(t)\|^2_{[L^2(\Omega_2)]^2} - (uc_b(t), \nabla c_b(t))_{[L^2(\Omega_2)]^2} + (F_b(t)c_b(t), c_b(t))_{L^2(\Omega_2)}.$$

As we also have

$$-(uc_b(t), \nabla c_b(t))_{[L^2(\Omega_2)]^2} = -\frac{u_0}{2}\int_{\partial\Omega_{2,r\uparrow}} c_b^2(t)ds - \frac{u_0}{2}\int_{\partial\Omega_{1,2\downarrow}} c_b^2(t)ds,$$

then, taking into account the boundary condition for c_b on $\partial\Omega_{2,r}$, we deduce successively

$$\begin{aligned}\frac{1}{2}\frac{d}{dt}\|c_b(t)\|^2_{L^2(\Omega_2)} &= \int_{\partial\Omega_{1,2\downarrow}} -J_{c_b}(t).\eta_2 c_b(t)ds + \alpha_b\int_{\partial\Omega_{2,r\uparrow}} c_{b,ext}(t)c_b(t)ds \\ &\quad - \frac{u_0}{2}\int_{\partial\Omega_{2,r\uparrow}} c_b^2(t)ds - \frac{u_0}{2}\int_{\partial\Omega_{1,2\downarrow}} c_b^2(t)ds \\ &\quad - D_{b2}\|\nabla c_b(t)\|^2_{[L^2(\Omega_2)]^2} + (F_b(t)c_b(t), c_b(t))_{L^2(\Omega_2)} \\ &\le \int_{\partial\Omega_{1,2\downarrow}} -J_{c_b}(t).\eta_2 c_b(t)ds + \frac{\alpha_b^2}{4\delta^2}\int_{\partial\Omega_{2,r\uparrow}} c_{b,ext}^2(t)ds - D_{b2}\|\nabla c_b(t)\|^2_{[L^2(\Omega_2)]^2} \\ &\quad + (F_b(t)c_b(t), c_b(t))_{L^2(\Omega_2)} + \Big(\delta^2 - \frac{u_0}{2}\Big)\int_{\partial\Omega_{2,r\uparrow}} c_b^2(t)ds - \frac{u_0}{2}\int_{\partial\Omega_{1,2\downarrow}} c_b^2(t)ds,\end{aligned}$$

where $\delta \neq 0$ is an arbitrary constant.

Using the trace inequality

$$\|c_b(t)\|^2_{L^2(\partial\Omega_2)} \le T_r\Big(\|c_b(t)\|^2_{L^2(\Omega_2)} + \|\nabla c_b(t)\|^2_{[L^2(\Omega_2)]^2}\Big),$$

we obtain

$$\begin{aligned}&\frac{1}{2}\frac{d}{dt}\|c_b(t)\|^2_{L^2(\Omega_2)} \\ &\le \int_{\partial\Omega_{1,2\downarrow}} -J_{c_b}(t).\eta_2 c_b(t)ds + \Big(-D_{b2} + \Big(\delta^2 - \frac{u_0}{2}\Big)T_r + \frac{u_0}{2}T_r\Big)\|\nabla c_b(t)\|^2_{[L^2(\Omega_2)]^2} \\ &\quad + \Big(\Big(\delta^2 - \frac{u_0}{2}\Big)T_r + \frac{u_0}{2}T_r\Big)\|c_b(t)\|^2_{L^2(\Omega_2)} + (F_b(t)c_b(t), c_b(t))_{L^2(\Omega_2)} \\ &\quad + \frac{\alpha_b^2}{4\delta^2}\int_{\partial\Omega_{2,r\uparrow}} c_{b,ext}^2(t)ds;\end{aligned}$$

that is,

(17)
$$\frac{1}{2}\frac{d}{dt}\|c_b(t)\|^2_{L^2(\Omega_2)} \leq \int_{\partial\Omega_{1,2}\downarrow} -J_{c_b}(t).\eta_2 c_b(t)ds + \big(-D_{b2}+\delta^2 T_r\big)\|\nabla c_b(t)\|^2_{[L^2(\Omega_2)]^2} + \delta^2 T_r\|c_b(t)\|^2_{L^2(\Omega_2)} + (F_b(t)c_b(t),c_b(t))_{L^2(\Omega_2)} + \frac{\alpha_b^2}{4\delta^2}\int_{\partial\Omega_{2,r}\uparrow} c^2_{b,ext}(t)ds.$$

In the previous inequality δ satisfies $\delta^2 > u_0$. From (16) and (17), taking into account the continuity of $c_b(t)$ on $\partial\Omega_{1,2}$, the interface condition for the bacterial fluxes on the interface $\partial\Omega_{1,2}$ and the fact that the line integral does not depend on path directions, we get

(18)
$$\frac{1}{2}\frac{d}{dt}\|c_b(t)\|^2_{L^2(\Omega)} + \min\{D_{b1}, D_{b2}-\delta^2 T_r\}\|\nabla c_b(t)\|^2_{[L^2(\Omega)]^2} \leq (F_b(t)c_b(t),c_b(t))_{L^2(\Omega)} + \delta^2 T_r\|c_b(t)\|^2_{L^2(\Omega_2)} + \frac{\alpha_b^2}{4\delta^2}\int_{\partial\Omega_{2,r}\uparrow} c^2_{b,ext}(t)ds.$$

Then taking into account that $c_{b,i}(t) \geq 0, i = 1, 2$, we obtain

$$\begin{aligned}(F_b(t)c_b(t),c_b(t))_{L^2(\Omega)} &= \sum_{i=1}^{2}\int_{\Omega_i}\left(E_0\left(1-\frac{c_{b,i}(t)}{c_{b,max}}\right) - E_{max}e^{-\beta_b t}\frac{c_{d,i}}{c_{50}+c_{d,i}}\right)c^2_{b,i}d\omega \\ &\leq \sum_{i=1}^{2}\left(E_0 - E_{max}e^{-\beta_b T_f}\frac{\bar{c}_{d,i}}{c_{50}+\bar{c}_{d,i}}\right)\|c_{b,i}(t)\|^2_{L^2(\Omega_i)} \\ &\leq \max_{i=1,2}\left(E_0 - e^{-\beta_b T_f}E_{max}\frac{\bar{c}_{d,i}}{c_{50}+\bar{c}_{d,i}}\right)\|c_b(t)\|^2_{L^2(\Omega)}.\end{aligned}$$

Considering the last upper bound in (18) we deduce

(19)
$$\frac{1}{2}\frac{d}{dt}\|c_b(t)\|^2_{L^2(\Omega)} + \min\{D_{b1}, D_{b2}-\delta^2 T_r\}\|\nabla c_b(t)\|^2_{[L^2(\Omega)]^2} \leq \frac{\alpha_b^2}{4\delta^2}\int_{\partial\Omega_{2,r}\uparrow} c^2_{b,ext}(t)ds + \theta\|c_b(t)\|^2_{L^2(\Omega_2)},\ t\in(0,T_f],$$

with

$$\theta = \delta^2 T_r + \max_{i=1,2}\left(E_0 - E_{max}e^{-\beta_b T_f}\frac{\bar{c}_{d,i}}{c_{50}+\bar{c}_{d,i}}\right). \tag{20}$$

Inequality (19) leads to the result present in Proposition 3.2.

REFERENCES

[1] P. Ankomah, P. J. T. Johnson, and B. R. Levin, *The pharmaco - population and evolutionary dynamics of multi-drug therapy: Experiments with S. aureus and E. coli and computer simulations*, PLoS Pathog., 9 (2013), pp. 1–14, e1003300.

[2] D. J. Austin and R. M. Anderson, *Studies of antibiotic resistance within the patient, hospitals and the community using simple mathematical models*, Philosophical Trans. Roy. Soc., 354 (1999), pp. 721–738.

[3] D. A. Jones, H. L. Smith, Le Dung, and M. Ballyk, *Effects of random motility on microbial growth and competition in a flow reactor*, SIAM J. Appl. Math., 59 (1998), pp. 573–596.

[4] D. Begic, C. V. Eiff, and B. T Tsuji, *Daptomycin pharmacodynamics against Staphylococcus aureus hemB mutants displaying the small colony variant phenotype*, J. Antimicrob Chemother, 63 (2009), pp. 977–981.

[5] H. Berg, *Random Walks in Biology*, Princeton University Press, Princeton, 1993.
[6] R. Bernardes, J. A. Ferreira, M. Grassi, M. Nhangumbe, and P. de Oliveira, *Fighting opportunistic bacteria in drug delivery medical devices*, SIAM J. Appl. Math., 79 (2019), pp. 2456–2478.
[7] S. L. Chua, J. K. H. Yam, P. Hao, S. S. Adav, M. M. Salido, Y. Liu, M. Givskov, S. K. Sze, T. Tolker-Nielsen, and L. Yang, *Selective labelling and eradication of antibiotictolerant bacterial populations in Pseudomonas aeruginosa biofilms*, Nature Commun. 7 (2016), 10750.
[8] R. O. Darouiche, *Treatment of infections associated with surgical implants*, New England J. Med., 350 (2004), pp. 1422–1429.
[9] E. S. Daus, J. P. Milisic, and N. Zamponi, *Analysis of a degenerate and singular volume-filling cross-diffusion system modeling biofilm growth*, SIAM J. Math. Anal., 51 (2019), pp. 3569–3605.
[10] N. Dror, M. Mandel, Z. Hazan, and G. Lavie, *Advances in microbial biofilm prevention on indwelling medical devices with emphasis on usage of acoustic energy*, Sensors, 9 (2009), pp. 2538–2554.
[11] J. A. Ferreira, P. de Oliveira, and P. M. Silva, *Computational simulation of bacterial infections in surgical procedures: An exploratory study*, in Springer Proceedings in Mathematics & Statistics 333, Springer, New York, 2020.
[12] A. Fuentes-Hernández, A. Hernández-Koutoucheva, A. F. Muñoz, R. D. Palestino, and R. Peña-Miller, *Diffusion-driven enhancement of the antibiotic resistance selection window*, J. Roy. Soc. Interface, 16 (2019), pp. 1–12.
[13] R. Gesztelyi, J. Zsuga, A. Kemeny-Beke, B. Varga, B. Juhasz, and A. Tosaki, *The Hill equation and the origin of quantitative pharmacology*, Arch. History Exact Sci., 66 (2012), pp. 427–438.
[14] D. Gutiérrez, C. Hidalgo-Cantabrana, A. Rodríguez, P. García, and P. Ruas-Madiedo, *Monitoring in real time the formation and removal of biofilms from clinical related pathogens using an impedance-based technology*, PLoS Pathog., (2016), pp. 1–17, e0163966.
[15] Y. J. Ki, K. W. Park, J. Kang, C. H. Kim, J. K. Han, H. M. Yang, H. J Kang, B. K. Koo, and H. S. Kim, *Safety and efficacy of second-generation drug-eluting stents in real-world practice: Insights from the multicenter grand-DES registry*, J. Intervent. Cardio., (2020), 3872704.
[16] O. Kindler, O. Pulkkinen, A. G. Cherstvy, and R. Metzler, *Burst statistics in an early biofilm quorum sensing model: The role of spatial colony-growth heterogeneity*, Sci. Reports, 9 (2019), pp. 1–19.
[17] G. Li, L. Tam, and J. X. Tang, *Amplified effect of Brownian motion in bacterial near-surface swimming*, Proc. Nat. Acad. Sci. USA, 105 (2008), pp. 18355-18359.
[18] L. Liu, H. Shi, H. Yu, S. Yan, and S. Luan, *The recent advances in surface antibacterial strategies for biomedical catheters*, Biomaterials Sci., 8 (2020), pp. 4095–4108.
[19] C. A. Lorenzo and A. Concheiro, *Smart drug release from medical devices*, J. Pharmacology and Experimental Therapeutics, 370 (2019). pp. 544–554.
[20] T. F. Mah, *Biofilm-specific antibiotic resistance*, Future Microbiology, 7 (2012), pp. 1061–1072.
[21] G. Melaugh, J. Hutchison, K. N. Kragh, Y. Irie, A. Roberts, T. Bjarnsholt, S. P. Diggle, V. D. Gordon, and R. J. Allen, *Shaping the growth behaviour of biofilms initiated from bacterial aggregates*, PLoS One, 11 (2016), pp. 1–18.
[22] L. Pisani, *Simple expression for the tortuosity of porous media*, Transport in Porous Media, 88 (2011), pp. 193–203.
[23] C. Potera, *Antibiotic resistance: Biofilm dispersing agent rejuvenates older antibiotics*, Environmental Health Perspectives, 118 (2010), pp. 288–291.
[24] R. R. Regoes, C. Wiuff, R. M. Zappala, K. N. Garner, F. Baquero, and B. R. Levin, *Pharmacodynamic functions: A multiparameter approach to the design of antibiotic treatment regimens*, Antimicrobial Agents and Chemotherapy, 48 (2004), pp. 3670–3676.
[25] R. Schulz and P. Knabner, *An effective model for biofilm growth made by chemotactical bacteria in evolving porous media*, SIAM J. Appl. Math., 77 (2017), pp. 1653–1677.
[26] S. Sharma and R. Steuer, *Modelling microbial communities using biochemical resource allocation analysis*, J. Roy. Soc. Interface, 16 (2019), pp. 1–15.
[27] J. Siepmann and F. Siepmann, *Modeling of diffusion controlled drug delivery*, J. Controlled Release, 161 (2012), pp. 351–362.
[28] C. Spalding, E. Keen, D.J. Smith, A. M. Krachler, and S. Jabbari, *Mathematical modelling of the antibiotic-induced morphological transition of Pseudomonas aeruginosa*, PLoS Comput. Biol., 14 (2018), e1006012.
[29] P. S. Stewart, *Mechanisms of antibiotic resistance in bacterial biofilms*, Int. J. Med. Microbiol., 292 (2002), pp. 107–113.
[30] P. S. Stewart, *Antimicrobial tolerance in biofilms*, Microbiol Spectr., 3 (2015).
[31] K. Vasilev, J. Cook, and H. J. Griesser, *Antibacterial surfaces for biomedical devices*, Expert Rev. Med. Devices, 6 (2009), pp. 553–67.

[32] M. Viceconti, A. Henney, and E. Morley-Fletcher, *In silico clinical trials: How computer simulation will transform the biomedical industry*, Int. J. Clinical Trials, 2 (2016), pp. 37–46.
[33] M. Youle, F. Rohwer, and A. Stacy, *The microbial olympics*, Nat. Rev. Microbiol., 10 (2012), pp. 583–588.
[34] X. Zhu and R. D. Braatz, *A mechanistic model for drug release in PLGA biodegradable stent coatings coupled with polymer degradation and erosion*, J. Biomed. Materials Res., Part A, 103 (2015), pp. 2269–79.